# Towards High-Fidelity Analysis on Wheeled Mobile Robot on Soft Terrain Using Hardware-in-the-Loop Simulator

Sora Ishikawa and Genya Ishigami



September 29, 2021

# TOWARDS HIGH-FIDELITY ANALYSIS ON WHEELED MOBILE ROBOT ON SOFT TERRAIN USING HARDWARE-IN-THE-LOOP SIMULATOR

**Sora Ishikawa and Genya Ishigami**

*Department of Mechanical Engineering, Keio University, Yokohama, Japan*
soraishikawa@keio.jp , ishigami@mech.keio.ac.jp

**Abstract**

This paper introduces a Hardware-In-the-Loop Simulation (HILS) framework for a wheeled mobile robot traveling on sandy terrain. The HILS is a hybrid method that incorporates an experimental approach into a numerical simulation. The HILS in our work employs a single-wheel testbed for the experimental setup where the traction force of the wheel on soft soil under various slip conditions is measured. The dynamics of the robot vehicle in response to the wheel traction force is calculated by a simple dynamics model based on Newton's equation of motion. A key technique of the HILS developed in this work is the damping coefficient implemented in the dynamics model. To verify the fidelity and stability of the HILS, wheel driving tests with the HILS are conducted in the following process: first, a wheel driving data (wheel translational velocity, wheel traction force, and wheel slip) with various input parameters (damping coefficient and wheel angular velocity) is experimentally measured only using the wheel testbed. Subsequently, another wheel driving data is measured while the HILS calculates the dynamic response of the wheel in accordance with the corresponding external forces. The validity of the HILS is compared based on the difference between the actual and calculated wheel driving data. In this process, the value of the damping coefficient is determined such that the dynamic response well matches with the actual driving data. Furthermore, wheel driving data with external disturbances to the wheel is experimentally simulated using the HILS.

**Keywords:** Hardware-In-the-Loop Simulation, Planetary rover, Soft soil

## 1. Introduction

Planetary rovers are used to acquire detailed scientific data that are valuable for revealing the history of the planetary bodies as well as for identifying the proof of past/present life on the bodies. The rover needs to be adequately designed to traverse on the planetary surface because scientific data are often buried in challenging rough terrain. The most common approach for evaluating rover mobility in its design and development phase is to perform an experimental test with an actual rover testbed or to calculate the dynamic behavior of the rover using numerical simulation. These two approaches are subject to pros and cons in terms of their reliability and accuracy for the results. The experimental approach provides a reliable dataset that is used for verifying the rover design; however, it is time-consuming and cost-ineffective to perform many experimental trials. The simulation approach can execute a vast number of trials with various simulation conditions while it requires accurate vehicle dynamics and interaction models in rough terrain. Past researches in the Terramechanics proposed different models of the dynamics on soft soil; however, the accuracy of the models may be modest in different vehicles on various terrain.

A method called Hardware-In-the-Loop Simulation (HILS) has been widely employed to address the above-mentioned issues. The HILS synchronizes a part of the numerical simulation with the data obtained from an actual hardware experiment in real-time. The HILS has been used to verify control methods for automobiles, aircraft, and satellites (Shimoji 1990; Lee 2004; Bolien 2017; Yang 2018). Applying the HILS principle to a wheeled rover design theoretically enables a high-fidelity simulation of the rover. This is because the HILS directly measures the interaction mechanics of the wheel in rough terrain and calculates the behavior of the rover vehicle with a dynamic model of the rover. However, the HILS for the rover has not been well demonstrated yet, and therefore its effectiveness is still uncertain.

The main scope of this paper is to develop and to verify the HILS for a wheel driving on soft soil. In this work, the HILS with a single wheel testbed was developed for simplifying wheeled rover mobility on soft soil. The hardware test of the HILS measures the wheel-soil interaction force while the software simulation of the HILS calculates the dynamic response of a wheel with regard to the force measured at the hardware. Experimental trials with varied wheel traveling condition in the HILS confirms the fidelity and usefulness of the HILS developed in this work.

## 2. Overview of the HILS for wheel dynamics

### *2.1 Overview of the HILS*

Figure 1 shows a general framework of the HILS. As compared to a full software simulation for a target system, the HILS replaces a part of a numerical model of the system to an actual experiment using a hardware testbed. The hardware testbed of the HILS measures a real phenomenon of the part of the system in a hardware environment. Subsequently, in a software environment, the numerical model calculates a response of the system in terms of the measured values. The HILS continuously loops these experimental measurements and numerical calculations as the temporal behavior of the system progress. The HILS is particularly useful for a case where an actual phenomenon of a target system is hardly measurable or another case where an accurate numerical model is barely available.

Given that the usefulness of the HILS, we employ the HILS for a rover mobility analysis. The hardware of the HILS measures the interaction force of a wheel on soft soil while the simulation calculates the dynamic behavior of a wheeled rover. The next subsection describes the framework of the HILS developed in our work.

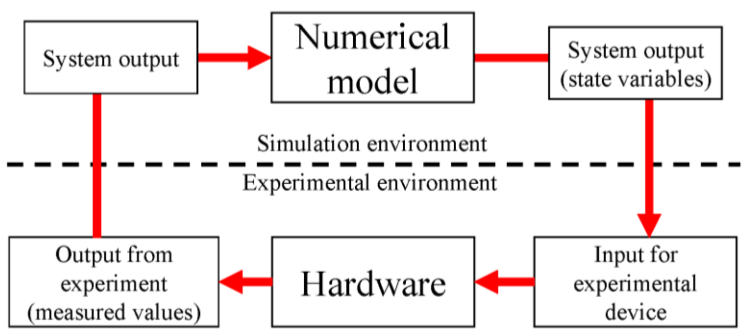


*Fig. 1. Schematic view of Hardware-In-the-Loop Simulation*

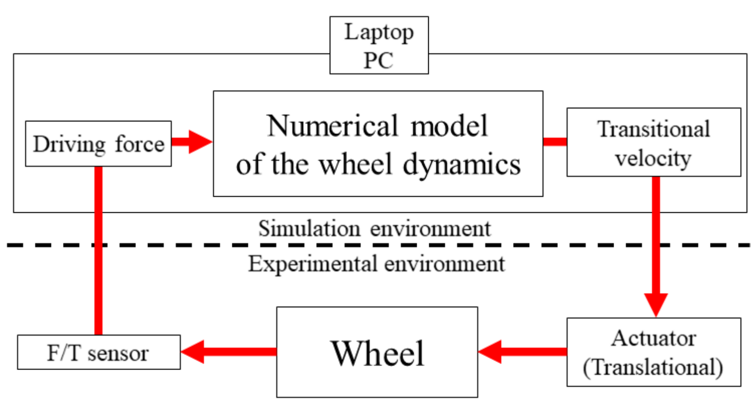


*Fig. 2. Schematic framework of the single wheel HIL*

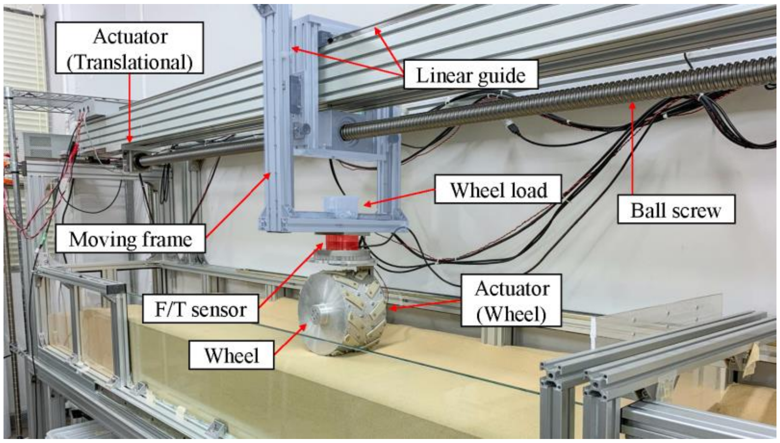


*Fig. 3. Single-wheel testbed overview*

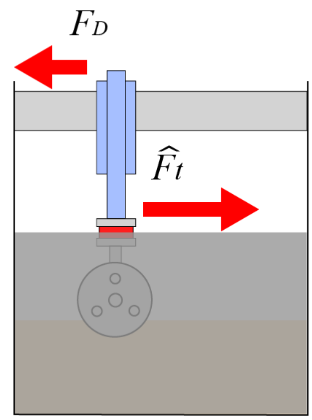


*Fig. 4. Forces on moving frame*

**Table. 1.** Parameters used for the hardware of the HILS

| | |
|---|---|
| Frictional force $F_D$ | 4.33 N |
| Mass $m$ | 10 kg |
| Sampling rate $\Delta t$ | 0.10 s |
| Damping coefficient $d$ | 0.994 |

## *2.2 Development of the Single wheel HILS*

Figure 2 illustrates the framework of the single wheel HILS developed in this work. Here, we focus on a wheel dynamics on soft soil. The simulation environment calculates the forward dynamics of the wheel using the actual measurement of the wheel force. In the experiment with the single wheel testbed (Fig. 3), the translational velocity of the wheel is controlled in accordance with the output from the result of the forward dynamics. The wheel force measured by the testbed is then fed to the simulation environment. Each loop of the HILS framework runs at an interval of 0.1 seconds.

### *2.2.1 Hardware setup of the HILS*

The single-wheel testbed is filled with Toyoura sand as soft soil. The wheel angular velocity is controlled by an actuator installed inside the wheel. The wheel linear velocity is also controlled by the translational actuator via a ball screw, while its vertical motion is free along with the linear guide. Controlling the translational actuator with regard to the wheel angular velocity achieves an arbitrary wheel slip. Further, detaching the ball screw from the horizontal linear guide, the wheel is self-propelled by its driving force. In this study, we define this driving as a "self-propelled drive."

A force-torque sensor (FPS080YS102U6S, Leptrino Co.) mounted on the upper part of the wheel measures the wheel driving force. The magnetic scales installed on the linear guides measure the horizontal and vertical displacements of the wheel, respectively.

### *2.2.2 Simulation model of the HILS*

The forward dynamics of the numerical model of the wheel provide the translational velocity of the wheel. In this study, a simple dynamics model is used as the numerical model to calculate the translational velocity in response to the measured driving force. As shown in Fig. 4, the force acting on the moving frame $F_t$ at an arbitrary time step $t$ is the resultant force coupled with the wheel driving force $\hat{F}_t$ and the constant resistive force on the horizontal linear guide $F_D$:

$$F_t = \hat{F}_t - F_D \tag{1}$$

Given *m* as the wheel mass, the simple dynamics model based on Newton's equation of motion derives the wheel linear acceleration $a_t$:

$$a_t = \frac{F_t}{m} \tag{2}$$

Subsequently, the translational velocity at time *t*, namely $v_t$, is calculated using sampling interval $\Delta t$ the first-order time integral:

$$v_t = v_{t-1} + a_t \Delta t - d(v_{t-1} - v_{t-2}) \tag{3}$$

where $d$ is the damping coefficient for the dynamic system. This is because the HILS usually introduces such a damping term between the hardware and software framework so that the hardware experiment becomes stable. The value of the damping coefficient is experimentally determined by increasing $d$ until the HILS becomes nearly critical damping. The values of each parameter in this study are summarized in Table. 1.

## 3. Experiments for verification of the single-wheel HILS

### *3.1 Experiment 1 - normal traveling*

Experiment 1 verifies the single-wheel HILS system by comparing the wheel driving behavior given by the HILS with the actual wheel driving. The ball screws of the testbed is attached to the translational actuator for the HILS test while it is detached for the actual wheel driving (self-propelled drive). The wheel angular velocity was set at 10°/s.

Figure 5 and Table 2 summarize the results of Experiment 1. At the steady state, the average error between the HILS-based output and the actual one is 5.39%, which indicates that the HILS well reproduces the actual traveling at steady-state condition.

On the other hand, the acceleration/deceleration of the wheel in the HILS was more gradual than those in the actual motion. This difference is due to the damping coefficient $d$: The large value for *d* caused the significant delay in response to the translational velocity. The actual force measured by the force-torque sensor was 2.55 N while the force using the HILS was 25.02 N, which was remarkablely large. Such a large force in the HILS then provides large acceleration of the wheel, resulting in the unstable motion of the single-wheel testbed. Therefore, the value of the damping coefficient need to be large enough to suppress the unstable motion.

On the other hand, the significant vibration is observed after the wheel braking. This is because that the translational actuator did not immediately produce the braking force to the wheel just after the rotational speed was set to $0\ \mathrm{m/s}$.

**Table. 2.** Results when the traveling is stable

| | Actual | HILS |
|---|---|---|
| Average velocity | $1.56 \times 10^{-2}$ m/s | $1.58 \times 10^{-2}$ m/s |
| Average of relative error | 5.39 % | |
| Maximum driving force at $t = \Delta t$ | 2.55 N | 25.02 N |

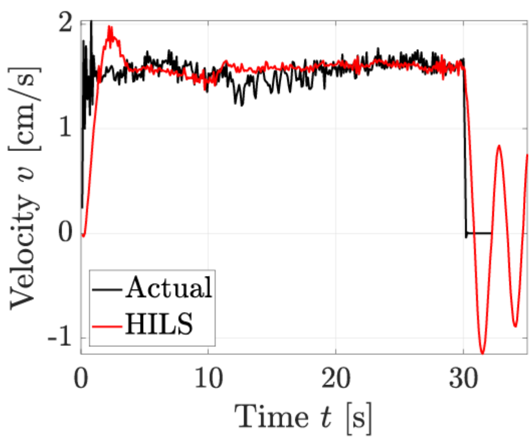


*Fig. 5. Experiment 1: wheel velocity profile of actual and HILS*

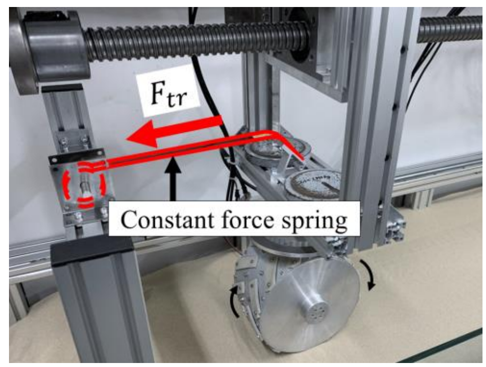


*Fig. 6. Overview of Experiment 2*

### *3.2 Experiment 2 – wheel drive with traction load*

In Experiment 2, a traction load $F_{tr}$ was applied under the same conditions in Experiment 1. In the actual driving, a constant force spring was attached to apply several arbitrary traction loads to the wheel (Fig. 6). The following constant force springs were respectively tested: 3.9 N, 9.8 N, 19.6 N, 28.4 N, 38.3 N, and 46.1 N. For the HILS driving, a virtual traction load $F_{vir}$ for simulating virtual constant force is added to Eq. 1 as follows:

$$F_t = \hat{F}_t - F_D - F_{vir} \tag{6}$$

Figures 7 shows the time histories of the translation velocity with varied traction loads. The velocity measured in the HILS well match with that in the actual driving in the steady-state. On the other hand, under large traction loads such as 28.4 N and 46.1 N, the translational velocity of the HILS vibrates significantly.

Figure 8 shows the time histories of the wheel sinkage as the position of the wheel is plotted every 30 seconds. The HILS was able to simulate the tendency of the sinkage trajectory of the actual driving. However, immediately after the HILS starts, the sinkages of the HILS were slightly deeper than the actual ones. This is because the inertial force of the linear guide with the ball screw is relatively large and acts as the additional traction load for the wheel.

Furthermore, the wheel sinkages under the HILS were smaller than the actual sinkage. It is assumed that the force $F_D$ from the slide guide increases as increasing the moment applied to the moving frame from the constant force spring.

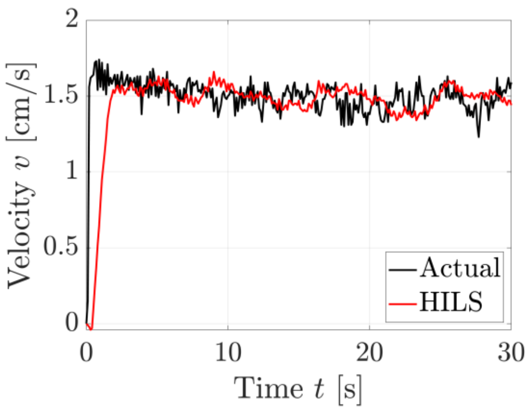


*(a)* $F_{tr}$ & $F_{vir}$ = 3.9 N

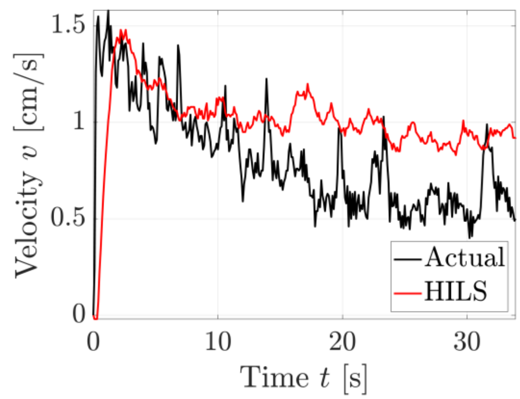


*(b)* $F_{tr}$ & $F_{vir}$ = 9.8 N

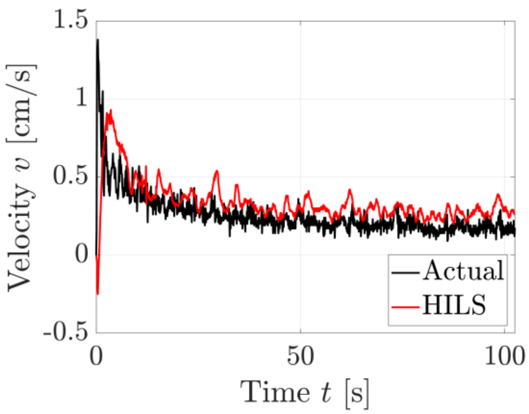


*(c)* $F_{tr}$ & $F_{vir}$ = 19.6 N

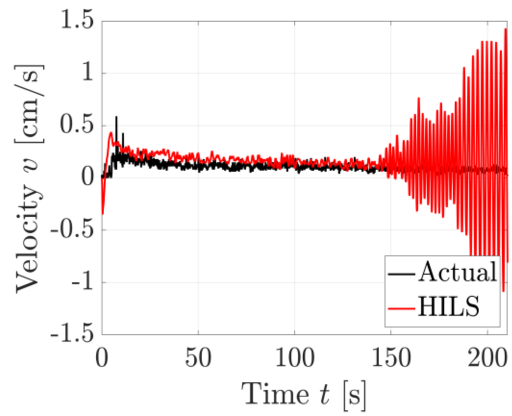


*(d)* $F_{tr}$ & $F_{vir}$ = 28.4 N

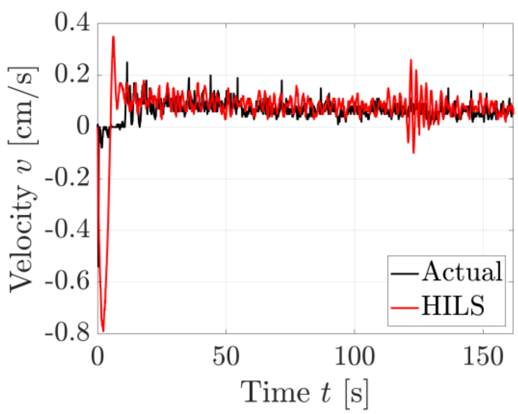


*(e)* $F_{tr}$ & $F_{vir}$ = 38.3 N

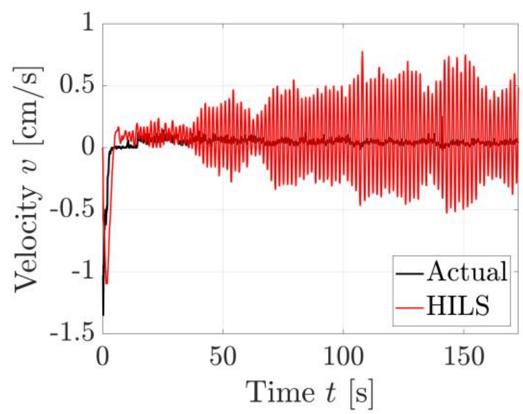


*(f)* $F_{tr}$ & $F_{vir}$ = 46.1 N

*Fig. 7. Time history of the translational velocity in actual and HILS test with varied traction loads*

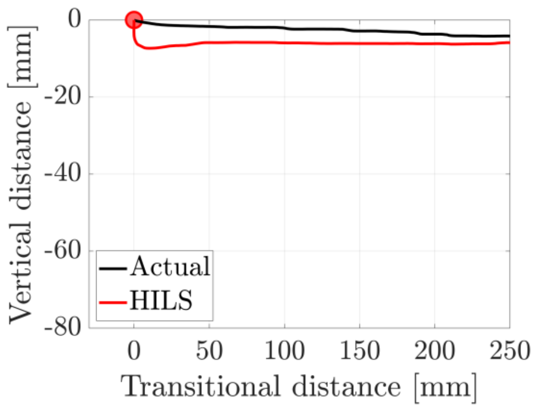


*(a)* $F_{tr}$ & $F_{vir}$ = 3.9 N

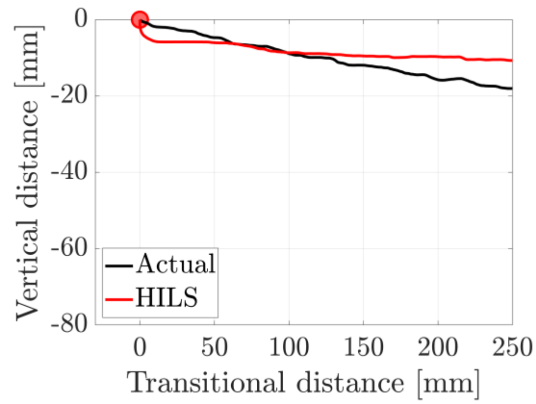


*(b)* $F_{tr}$ & $F_{vir}$ = 9.8 N

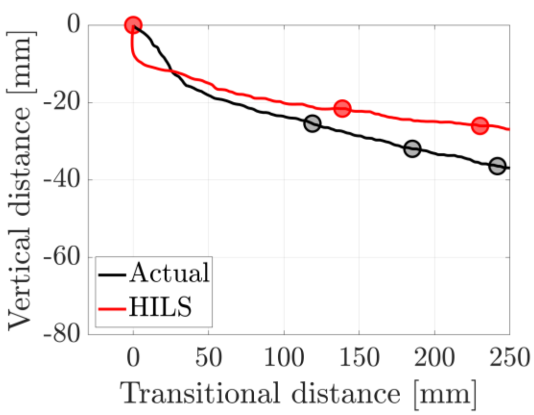


*(c)* $F_{tr}$ & $F_{vir}$ = 19.6 N

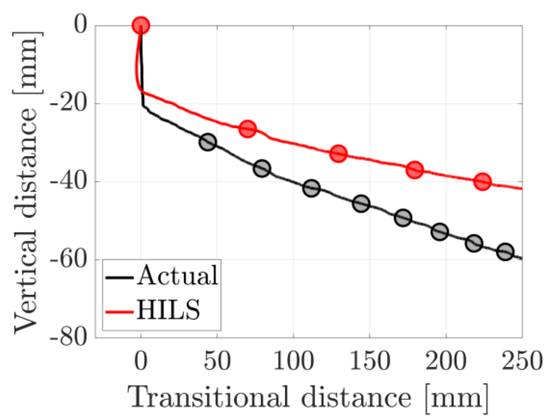


*(d)* $F_{tr}$ & $F_{vir}$ = 28.4 N

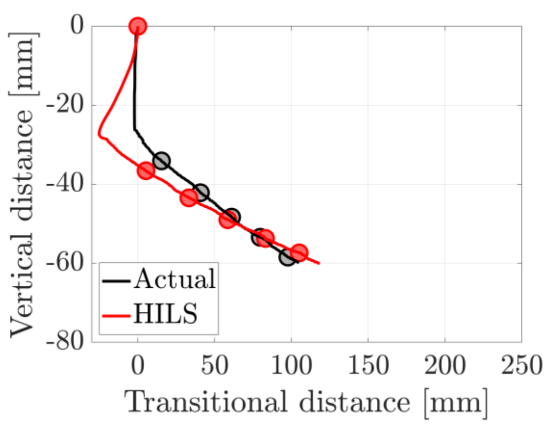


*(e)* $F_{tr}$ & $F_{vir}$ = 38.3 N

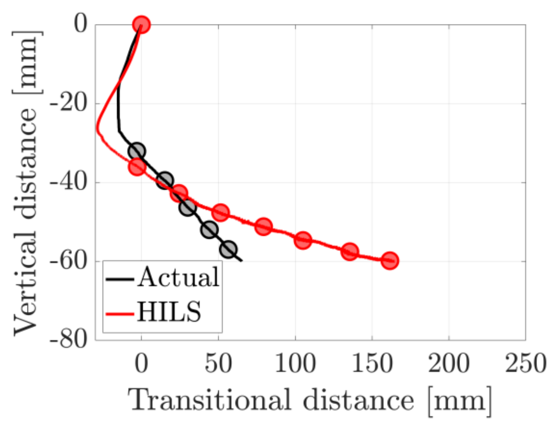


*(f)* $F_{tr}$ & $F_{vir}$ = 46.1 N

*Fig. 8. Time history of the wheel sinking trajectory in actual and HILS tests with varied traction loads*

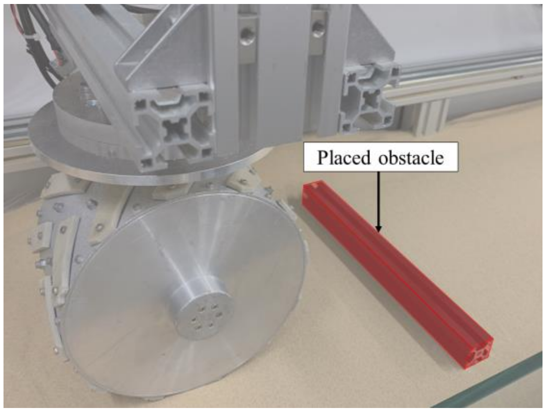


(a) Condition 1

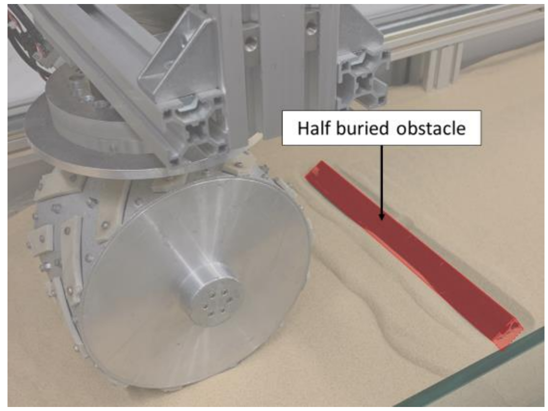


(b) Condition 2

*Fig. 9. Snapshots of obstacles in Experiment 3*

## 3.3 Experiment 3 – obstacle traverse

Experiment 3 investigated the behavior of a wheel dynamic response when the wheel traverses a rigid obstacle. An aluminum frame having a dimension of $30 \times 30 \times 320$ mm was put in front of the wheel path with the following two conditions:

- Condition 1: The obstacle is placed on soft soil surface (Fig. 9 (a))
- Condition 2: The obstacle is half buried in soft soil (Fig. 9 (b))

Figure 10 summarizes the results of the translational velocities of the actual and HILS traveling in each condition. Figure 11 illustrates the wheel driving process that was commonly observed when the wheel traversed the obstacle. The velocity decreased immediately after the contact with the obstacle (Fig. 11(b)) and increased at the moment of sliding down the obstacle (Fig. 11(d)). As compared to the velocity profile of the actual driving, the velocity of the HILS did not show large spikes during the test. This is because the damping coefficient in the equation of motion in the HILS surpressed the dynamic change of the velocity.

Regarding this gradual change in the HILS, we conclude that the HILS is not able to address impulsive forces that occur in a moment shorter than the sampling interval of the HILS.

## 3.4 Experiment 4 – parameter dependency

Experiment 4 was conducted with varied wheel angular velocity and damping coefficient such that the dynamic response of the HILS with regard to those parameters is confirmed. The wheel angular velocity was set as $\omega = 5°/s$ and $\omega = 15°/s$ , while the different damping coefficient was set as 0.990 with a step of 0.002.

Figure 12 shows the translational velocity of actual and HILS traveling at $\omega$ was $5°/s$ and $15°/s$ . Figure 12 also shows the translational velocity for each damping coefficient $d$. When the wheel rotational speed $\omega$ was $5°/s$, the velocity was almost equal to that of the actual driving at the steady state. Further, the effect of the damping coefficient of the HILS is theoretically consistent; the overshoot at the transient state decreases as increasing the damping coefficient, and the translational velocity converges quickly. On the other hand, for $\omega$ =15°/s, the value of the translation velocity at the steady-state varied along with varying damping coefficient. This is because the value of the coefficient is much larger than the critical damping of the system. From these results, we concluded that the damping coefficients must be appropriately tuned in realtime for the wheel angular velocity.

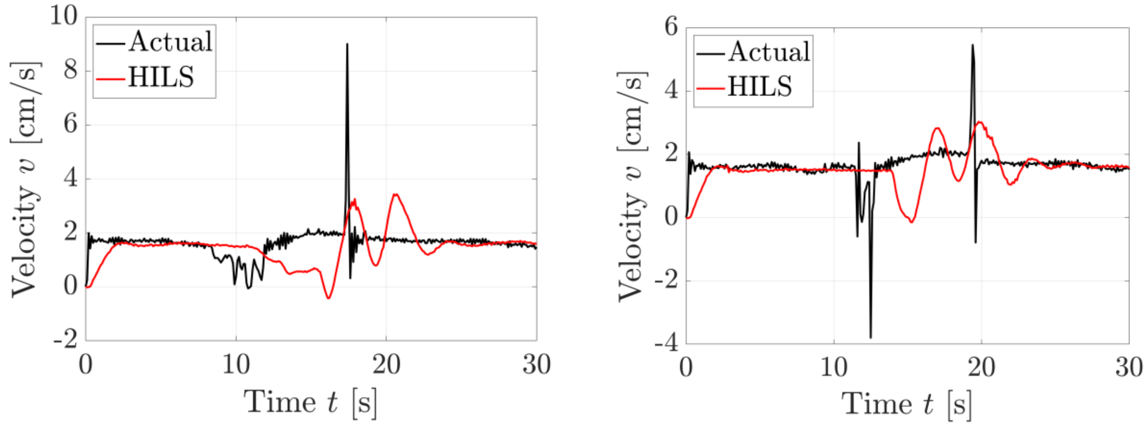


*(a) Condition 1* *(b) Condition 2*

*Fig. 10. Translational velocity profile for the obstacle traverse in Experiment 3*

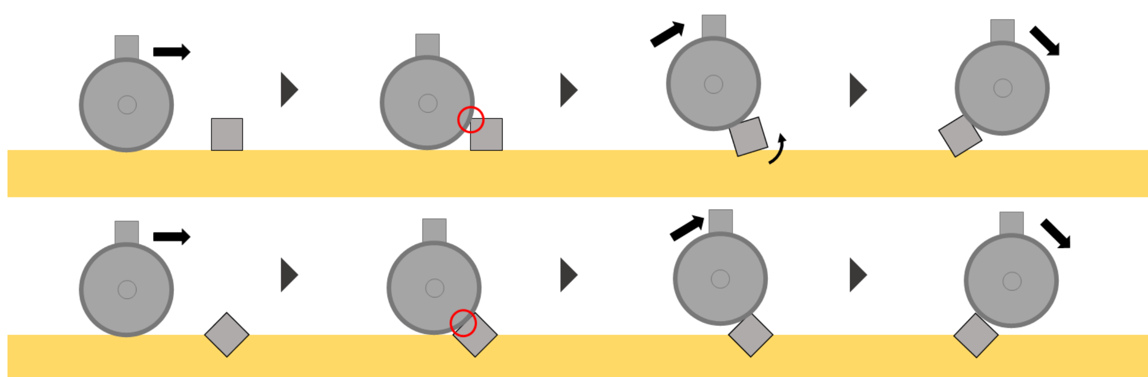

*(a) Travel on flat ground* *(b) Contact with an obstacle* *(c) Climb up the obstacle* *(d) Sliding down the obstacle*

*Fig. 11. The process of the wheel over an obstacle*

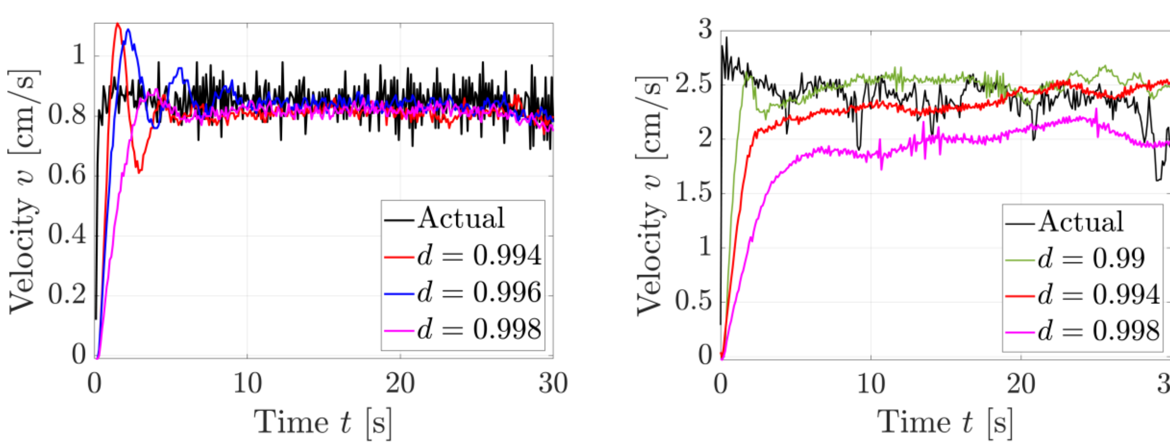


*(a) $\omega = 5°/s$* *(b) $\omega = 15°/s$*

*Fig. 12. Comparison with varied rotational speed $\omega$ and damping coefficient $d$*

## 4. Conclusion

In this study, we developed a HILS system using a single-wheel testbed with a simplified dynamics model. The HILS was experimentally examined under various conditions. The HILS was able to perform stable and high-fidelity simulations when traveling in a steady-state on flat and soft ground. The experiment also revealed that the system delay of the HILS highly depends on the damping coefficient introduced in the simplified dynamics model. The system delay degrades the fidelity of the HILS, particularly in the starting and braking motion of the wheel. Future works of the research include the realtime tuning of the damping coefficients and increment of the sampling rate.

## Nomenclature

| | | |
|---|---|---|
| $F_t$ | Net traction force | [N] |
| $\hat{F}_t$ | Traction force from wheel | [N] |
| $F_D$ | Resistance force from slide guide | [N] |
| $a_t$ | Acceleration in translation direction | $[\mathrm{m/s^2}]$ |
| $m$ | Mass of the moving frame | [kg] |
| $v_t$ | Velocity in translation direction | $[\mathrm{m/s}]$ |
| $\Delta t$ | Sampling rate | [s] |
| $d$ | Damping coefficient | [-] |
| $a_{est}$ | Calculated acceleration | $[\mathrm{m/s^2}]$ |
| $\Delta v$ | Velocity change | [m/s] |
| $F_{tr}$ | Traction load from constant force spring | [N] |
| $F_{vir}$ | Virtual traction load input to a model | [N] |

## Acknowledgements

This work was supported by JSPS KAKENHI Grant Number 18H01397.

## References

Shimoji, H., Inoue, M., Tsuchiya, K., Ninomiya, K., Nakatani, I., Kawaguchi, J, 1990,Simulation system for a space robot using 6 axis servos. Journal of the Robotics Society of Japan,Vol 8, 144–151.

Lee, K. C., Jeon, J. W., Hwang, D. H., Lee, S. H., Kim, Y. J., 2004. Development of antilock braking controller using hardware in-the-loop simulation and field test. IECON Proceedings,Vol 3, 2137–2141.

Bolien, M., Iravani, P., Du Bois, J. L., 2017, Toward robotic pseudodynamic testing for hybrid simulations of air-to-air refueling. IEEE/ASME Transactions on Mechatronics, Vol 22, 1004–1013.

Yang, J., Konno, A., Abiko, S., Uchiyama, M, 2018, Hardware-in-the-loop simulation of massive-payload manipulation on orbit. ROBOMECH Journal,Vol 5, 19-30.